BUREAU OF RECLAMATION

Desalination and Water Purification Research Program
Report No. 276

Synthesis of Novel Reverse Osmosis Separation Layers to Enhance the Rejection of Uncharged Molecules in Desalination

U.S. Department of the Interior **October 2022**

REPORT DOCUMENTATION PAGE

Form Approved
OMB No. 0704-0188

PLEASE DO NOT RETURN YOUR FORM TO THE ABOVE ADDRESS.

1. REPORT DATE *(DD-MM-YYYY)*	**2. REPORT TYPE**	**3. DATES COVERED** *(From - To)*
24-10-2022	Final	04/01/2020 – 09/30/2022

4. TITLE AND SUBTITLE
Synthesis of Novel Reverse Osmosis Separation Layers to Enhance the Rejection of Uncharged Molecules in Desalination

5a. CONTRACT NUMBER
Agreement Number R19AC00087

5b. GRANT NUMBER

5c. PROGRAM ELEMENT NUMBER

6. AUTHOR(S)
Dr. Steven T. Weinman, Assistant Professor, PI
Dr. Milad R. Esfahani, Assistant Professor, co-PI

5d. PROJECT NUMBER

5e. TASK NUMBER

5f. WORK UNIT NUMBER

7. PERFORMING ORGANIZATION NAME(S) AND ADDRESS(ES)
The University of Alabama
152 Rose Administration Building
Box 870104
Tuscaloosa, Alabama 35487-0104

8. PERFORMING ORGANIZATION REPORT NUMBER

9. SPONSORING/MONITORING AGENCY NAME(S) AND ADDRESS(ES)
U.S. Department of the Interior
Bureau of Reclamation
Denver Federal Center
PO Box 25007
Denver, CO 80225-0007

10. SPONSOR/MONITOR'S ACRONYM(S)
Reclamation

11. SPONSOR/MONITOR'S REPORT NUMBER(S)
DWPR Report No. 276

12. DISTRIBUTION/AVAILABILITY STATEMENT
Available from https://www.usbr.gov/research/dwpr/DWPR_Reports.html

13. SUPPLEMENTARY NOTE

14. ABSTRACT

Reverse osmosis (RO) membranes are the gold standard for water desalination. Even though RO membranes exhibit excellent performance rejecting monovalent and divalent salt ions, they do not reject small, neutral molecules, such as urea, to a level to produce potable water. This project focused on using new RO membrane chemistries and new RO membrane modification strategies to improve urea rejection. The results indicate that modification with amines and heat are a productive way to significantly enhance urea rejection.

15. SUBJECT TERMS
Reverse Osmosis; Urea; Polyamide; Carbodiimide

16. SECURITY CLASSIFICATION OF:			**17. LIMITATION OF ABSTRACT**	**18. NUMBER OF PAGES**	**19a. NAME OF RESPONSIBLE PERSON**
a. REPORT	**b. ABSTRACT**	**a. THIS PAGE**			Stephen Ogle
U	U	U			**19b. TELEPHONE NUMBER** *(Include area code)* (303) 445-2255

Desalination and Water Purification Research Program
Report No. 276

Synthesis of Novel Reverse Osmosis Separation Layers to Enhance the Rejection of Uncharged Molecules in Desalination

Prepared by:

Dr. Steven T. Weinman, PI
Dr. Milad R. Esfahani, co-PI
The University of Alabama

Prepared for:

Bureau of Reclamation under Agreement No. R19AC00087

U.S. Department of the Interior **October 2022**

Mission Statements

The U.S. Department of the Interior protects and manages the Nation's natural resources and cultural heritage; provides scientific and other information about those resources; honors its trust responsibilities or special commitments to American Indians, Alaska Natives, and affiliated Island Communities.

The mission of the Bureau of Reclamation is to manage, develop, and protect water and related resources in an environmentally and economically sound manner in the interest of the American public.

Acronyms and Abbreviations

ACS	American Chemical Society
ATR-FTIR	attenuated total reflectance Fourier-transform infrared spectroscopy
DAB	1,4-diaminobutane
DAH	1,6-diaminohexane
DAO	1,8-diaminooctane
DAP	1,3-diaminopropane
DI	deionized
EDC	1-(3-dimethylaminopropyl)-3-ethylcarbodiimide hydrochloride
HCl	hydrochloric acid
HEPES	4-(2-hydroxyethyl)piperazine-1-ethanesulfonic acid
IP	interfacial polymerization
KCl	potassium chloride
MES	2-morpholinoethanesulfonic acid
MOF	metal organic framework
MPD	m-phenylenediamine
NaCl	sodium chloride
NaOH	sodium hydroxide
NHS	n-hydroxysuccinimide
N/O	nitrogen-to-oxygen
PALS	positron annihilation lifetime spectroscopy
PEI	polyethylenimine
PTCA	1,2,3-propanetricarboxylic acid chloride
RO	reverse osmosis
SEM	scanning electron microscopy
TFC	thin-film composite
TMC	trimesoyl chloride
UV	ultraviolet
XPS	x-ray photoelectron spectroscopy

Symbols

≈	approximately
>	greater than
≥	greater than or equal to
<	less than
%	percent
±	plus or minus
®	registered trademark

Measurements

bar	metric unit of pressure exactly equal to 100 kiloPascals
°C	degrees Celsius
cm^{-1}	inverse centimeter
cm^2	square centimeter
eV	electronvolt
g	gram
g/mol	grams per mol
h	hour
K	degrees Kelvin
kDa	kilodalton
kV	kilovolt
L	liter
L*bar/(mol*K)	liter*bar/mol/degree Kelvin
$L/m^2/h$	liter/square meter/hour (LMH)
$L/m^2/h/bar$	liter/square meter/hour/bar
m	meter
M	molarity (mol/L)
mg/L	milligram per liter
min	minute
mL	milliliter
mm	millimeter
mM	millimolar exactly equal to 0.001 M
mol/L	moles per liter
$mol/(m^2*h)$	mol/square meter/hour
MPa	MegaPascal
ms	millisecond
nm	nanometer
N/O	nitrogen-to-oxygen
pA	picoampere
ppm	parts per million
psi	pounds per square inch
s	second
µL	microliter
µm	micrometer
wt%	weight percentage
w/v%	weight-per-volume percentage

Variables

A	membrane water permeance
C	concentration of NaCl or urea
C_f	feed concentration
C_p	permeate concentration
i	dissociation constant
J_s	solute flux
J_w	water flux
ΔP	difference in pressure between the feed and permeate
R	rejection
R_g	universal gas constant
T	testing solution temperature
$\Delta\pi$	difference in osmotic pressure between the retentate and permeate

Contents

Page

Executive Summary ES-1

1.0 Introduction 1
1.1 Project Background 1
1.1.1 Problem and Needs 2
1.1.2 Objectives 3
1.1.3 Previous Research 3
1.2 Project Overview 3
1.2.1 Overall Approach and Concepts 3
1.2.2 Overall Method 4
2.0 Technical Approach and Methods 5
2.1 Research Approach 5
2.1.1 Research Idea 5
2.1.2 Equations 7
2.2 Project Facility/Physical Apparatus 8
2.2.1 Design Criteria 8
2.2.2 Source Water 8
2.2.3 Setup 8
2.3 Methodology 9
2.3.1 Methods Used 9
2.3.2 Runs and Experiments Done 13
3.0 Results and Discussion 15
3.1 Results 15
3.1.1 RO Membrane Synthesis Review Paper 15
3.1.2 RO Membrane Support Layer Properties Review Paper 15
3.1.3 RO Membrane Control 15
3.1.4 New Chemistries 16
3.1.5 Polyamide Membrane Modification 16
3.2 Analysis 28
3.2.1 New Chemistries 28
3.2.2 Amine Modification 28
4.0 Conclusions 31
4.1 New Chemistries 31
4.2 Amine Modification 31
4.3 Challenges 31
4.4 Recommended Next Steps 32
5.0 References 33

Tables

Table Page

1 Summary of water types to challenge membranes 8
2 Acronyms for XLE membranes 11
3 Acronyms for BW30 membranes 12
4 XPS data of XLE and BW30 membranes 18

Figures

Figure Page

1 Molecular level view of a polyamide reverse osmosis membrane. 1
2 Schematic of overall project concept. 3
3 The IP reaction process to create a polyamide RO membrane. 5
4 The monomers used in the IP reaction to create a polyamide RO membrane. 6
5 The reaction schematic for modifying polyamide RO membranes with MPD. 6
6 Sterlitech test cell used to evaluate membrane performance. 9
7 ATR-FTIR spectra of XLE and BW30 membranes. 17
8 Water contact angle of XLE and BW30 membranes. 19
9 Zeta potential of XLE and BW30 membranes. 20
10 Water permeance, NaCl rejection, and urea rejection of XLE membranes. 22
11 Water permeance, NaCl rejection, and urea rejection of BW30 membranes. 23
12 NaCl and urea solute permeability of XLE and BW30 membranes. 24
13 ATR-FTIR spectra of linear amine modified XLE membranes. 25
14 NaCl rejection of linear-amine modified XLE membranes. 26
15 Urea rejection of linear-amine modified XLE membranes. 27
16 Water permeance and urea rejection of modified XLE membranes. 28

Executive Summary

Reverse osmosis (RO) membranes are the gold standard for water desalination. Even though RO membranes exhibit excellent performance rejecting monovalent and divalent salt ions, they do not reject small, neutral molecules, such as urea, to a level to produce potable water. Due to the fast, uncontrolled nature of the interfacial polymerization (IP) reaction, the polyamide layer contains both network and aggregate free volume holes (pores). Because urea rejection is dominated by the size exclusion mechanism, reducing the free volume to reduce the passage of the urea through the membrane is needed. To achieve this, we focused on two methods: (1) synthesize polyamide RO membranes using new chemistries and (2) modify polyamide RO membranes using amines. We tested the hypotheses that (1) the flexibility of linear monomers will decrease network pore size and increase cross-linking density in synthesized RO membranes and (2) using the carbodiimide activation chemistry will either (a) increase the cross-linking density, (b) fill in the free volume spaces, or (c) both. We used the linear monomers 1,3-diaminopropane and 1,2,3-propanetricarboxylic acid chloride in the IP reaction to test hypothesis No. 1. We used m-phenylenediamine, linear diamines, and polyamines to modify commercial RO membranes to test hypothesis No. 2. The results indicate that linear monomers are not suitable for polyamide RO membranes due to their fragility and instability. The results indicate that modification with amines and heat are a productive way to significantly enhance urea rejection. Future research needs to explore other chemistries for polyamide RO membrane modification, and fundamental studies are needed to understand the mechanism of improved performance.

1.0 Introduction

1.1 Project Background

Reverse osmosis (RO) membranes are the gold standard for water desalination and have been used for over three decades. Even though RO membranes reject monovalent and divalent salt ions well, they do not reject small, neutral molecules, such as urea, to a level to produce potable water. Current RO membranes can only reject urea and boric acid at approximately 70% (Yoon and Lueptow 2005). RO membranes are thin-film composites (TFCs) composed of three layers: a polyamide top layer, a polysulfone support middle layer, and a polyester nonwoven bottom layer. Typical RO membrane polyamide separation layers are made by the interfacial reaction between m-phenylenediamine (MPD) and trimesoyl chloride (TMC). RO separation layers are regarded to not contain pores but are considered a dense polymer layer. The "pores" of an RO membrane are considered to be the free volume or spaces between polymer chains. Figure 1 shows that due to the fast, uncontrolled nature of the IP reaction, the polyamide layer contains both network and aggregate free volume holes (pores). The solution-diffusion model used to model dense polymer layer molecule transport accounts for the free volume of the separation layer in the diffusivity and solubility variables. Because small, neutral molecule rejection is dominated by the size exclusion mechanism, reducing the free volume to reduce the passage of the urea through the membrane is needed. This project was conducted at The University of Alabama, in Tuscaloosa, Alabama led by Dr. Steven T. Weinman and Dr. Milad R. Esfahani in the Department of Chemical and Biological Engineering. This project was restricted to small, bench-scale studies.

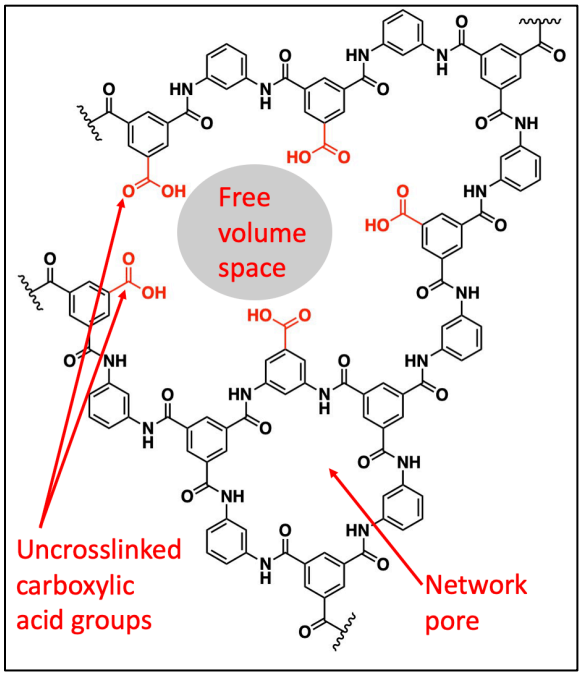

Figure 1.—Molecular level view of a polyamide RO membrane.

1.1.1 Problem and Needs

Urea, a nontoxic nitrogenous organic, is the end product of nitrogen metabolism that is discarded from the kidneys through urine. The human body produces 20–30 g of urea per day. In addition to mammalian protein metabolism, urea is the main component of more than 50% of global nitrogen-based fertilizer (Glibert et al. 2006). Anthropogenic urea may enter surface waters through different hydrologic pathways (Bogard et al. 2012), and around 40% of urea is exported to groundwater based on the type of fertilizer and irrigation methods used. Fertilization by urea, as a low-cost organic compound with high solubility in water, causes transport of urea to aquatic ecosystems. The demand for nitrogen-based fertilizer has increased 500% in the last 50 years due to human population increase and economic development all around the world (Finlay et al. 2010); therefore, urea entrance into the environment has different sources, such as wastewater of production plants, leaching from fields and agro-breeding farms, and as the final product of mammalian protein metabolism.

One of the direct effects of urea pollution is on ocean algae for the production of a deadly toxin called domoic acid (Schnetzer et al. 2007). The increased use of urea, and consequently the significant overland transport of urea to sensitive coastal waters, in the last few years, has resulted in the higher harmful algal bloom species that are responsible for wildlife death or human seafood poisonings. The acceptable urea concentration in waste streams is a maximum of 10 ppm, a decrease from 100 ppm used in the last decade. The reduction of allowed urea concentration from 100 to 10 ppm shows the current strict environmental legislation regarding urea removal (Rahimpour and Mottaghi 2009). There are different approaches to urea removal, including hydrolysis, enzymatic decomposition, catalytic decomposition, electrochemical oxidation, and adsorption; however, each of the mentioned approaches has limiting factors that hinder removal efficiency. The hydrolysis of urea should be performed at high temperatures (200–220 °C), high pressures (2–3 MPa), and high (> 2 h) residence times which has a high energy demand. The enzymatic decomposition of urea depends highly on the activity of the urease enzyme and operational conditions, such as pH and temperature, that limit this technique's applicability. Biological methods of urea removal use the power of microorganisms to decompose organic nitrogen to molecular nitrogen. The challenge of this method is determining the optimal conditions for biological degradation because of the complex behaviors of microorganisms. Physical adsorption using different adsorbents, such as activated carbon, polyethylenepolyamine/Cu(II) complex, and tolylene diisocyanate cross-linked β-cyclodextrin, were used for the removal of urea from water; however, lack of adsorption capacity and poor biocompatibility of the adsorbents limited the efficiency of the removal process (Liu et al. 2003). Although urea removal by catalytic decomposition showed noticeable performance, the cost of catalysis and providing the required operating conditions limit the removal process (Ananiev et al. 2003).

1.1.2 Objectives

The objectives of this research were to (1) use linear amine monomers in the IP reaction, (2) use linear acid chloride monomers in the IP reaction, (3) modify commercial RO membranes using MPD, and (4) modify commercial RO membranes using linear diamines and polyamines.

1.1.3 Previous Research

Previous research is not applicable to this project. This was the first project the Principal Investigator and co-Principal Investigator laboratories focused on studying the improvement of urea removal using polyamide RO membranes.

1.2 Project Overview

1.2.1 Overall Approach and Concepts

Our overall approach was to (1) identify and use new monomers for the interfacial polymerization (IP) process, (2) identify and use new amine chemistries for carbodiimide chemistry modification of RO membranes, and (3) characterize and performance evaluate synthesized and modified RO membranes. The overall general concept was to reduce the free volume element size of the polyamide RO membrane (essentially the pore size of the membrane) to increase the removal of the small, neutral molecule urea from water. Figure 2 shows the overall concept of the work done in this project.

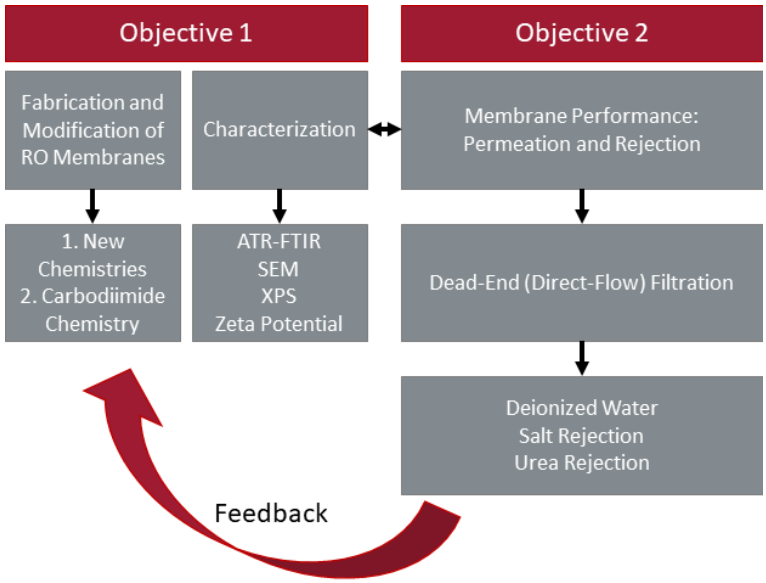

Figure 2.—Schematic of overall project concept.

1.2.2 Overall Method

The overall methods were to (1) synthesize new RO membranes and (2) modify commercial RO membranes to improve the rejection of urea. We characterized the synthesized and modified polyamide RO membranes with numerous methods to show successful synthesis and modification. We performance evaluated the membranes by challenging the membranes with deionized (DI) (pure water), sodium chloride (NaCl) (salt), and urea.

2.0 Technical Approach and Methods

2.1 Research Approach

2.1.1 Research Idea

In an attempt to reduce the free volume element size of the polyamide RO membranes, we used two basic ideas. Figure 3 shows the interfacial polymerization (IP) reaction. IP is a very fast reaction (< 1 min) between an aqueous amine monomer and an organic acid chloride monomer. The aqueous amine monomer diffuses into the organic phase and reacts instantaneously with the acid chloride monomer to form a polyamide network. As the reaction occurs, the diffusion diminishes due to the formation of the polyamide layer creating a semi-self-limiting reaction. The typical monomers used are MPD and TMC. These monomers are aromatic (ring structures containing double bonds) and, thus, are very rigid. Because this reaction is very fast, there is a distribution of areas where there is complete reaction (known as network pores) and areas where there is incomplete reaction (known as aggregate pores). Additionally, these aggregate pores of incomplete reaction contain free carboxylic acid groups (acid chlorides hydrolyze into carboxylic acids spontaneously upon contact with water) that are susceptible to reaction. The goals of this project were to (1) decrease the size of the network and aggregate pores by using linear monomers, which are able to rotate significantly more than MPD in the IP reaction and (2) fill in the aggregate pores with various amines using carbodiimide chemistry.

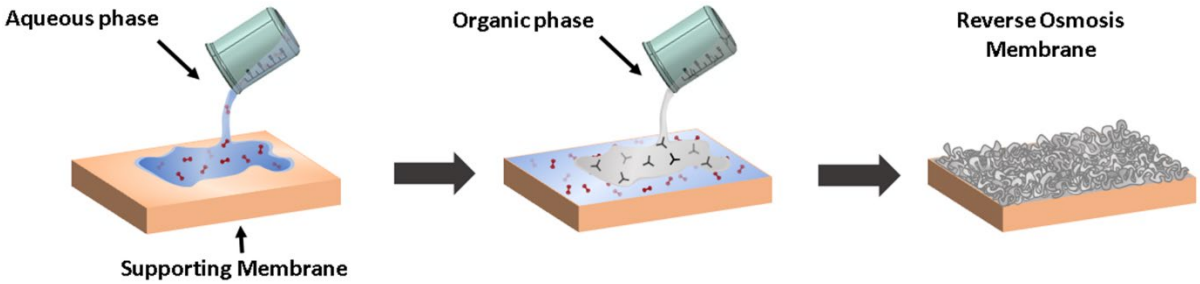

Figure 3.—The IP reaction process to create a polyamide RO membrane.

The first method we used was to use new linear monomers in the IP reaction. We investigated using 1,3-diaminopropane (DAP) as a linear amine monomer and 1,2,3-propanetricarboxylic acid chloride (PTCA) as a linear acid chloride monomer. Figure 4 shows the conventional MPD and TMC reactants, the DAP and TMC reactants, and the MPD and PTCA reactants that were tested. We initially made MPD and TMC membranes to ensure we could make adequate control membranes before we moved to testing the new chemistries.

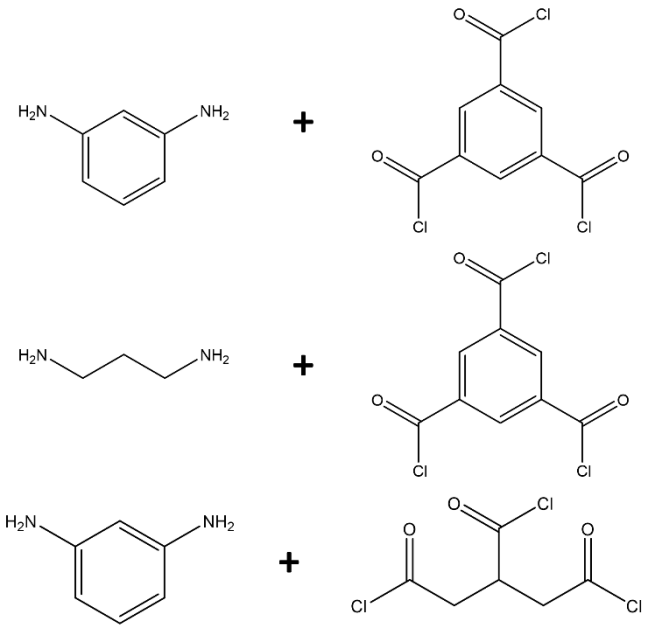

Figure 4.—The monomers used in the IP reaction to create a polyamide RO membrane.

The second method we used was to modify commercial RO membranes using carbodiimide chemistry. Carbodiimide chemistry uses 1-(3-dimethylaminopropyl)-3-ethylcarbodiimide hydrochloride (EDC) and n-hydroxysuccinimide (NHS) to activate the carboxylic acid groups to then form new amide bonds when exposed to primary amines. Figure 5 shows the initial reaction schematic used to modify polyamide RO membranes using MPD. We initially chose MPD to modify the membrane with the same chemistry it is made of. We also modified the membrane with linear diamines DAP, 1,6-diaminohexane (DAH), and 1,8-diaminooctane (DAO) and the polyamine polyethyleneimine (PEI) of two different molecular weights. We envisioned that the linear and polyamines have the ability to rotate more, thus filling in the gaps of the aggregate pores or finding another carboxylic acid group to anchor to, creating a new crosslink.

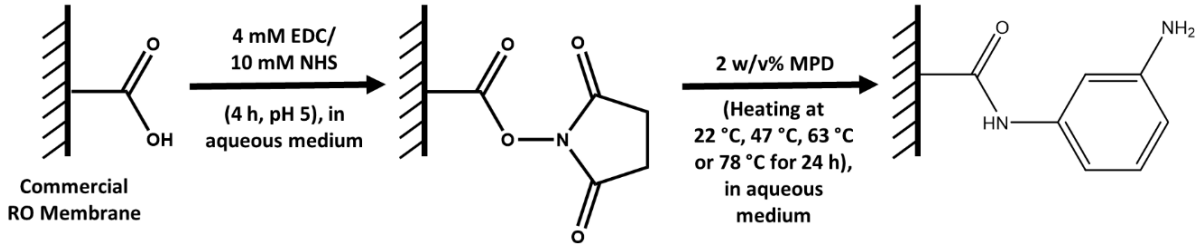

Figure 5.—The reaction schematic for modifying polyamide RO membranes with MPD.

We performed numerous characterizations on the synthesized and modified membranes, including attenuated total reflectance Fourier-transform infrared spectroscopy (ATR-FTIR) to investigate the functional groups of the membranes, scanning electron microscopy (SEM) to image the top surface of the membranes, streaming or zeta potential analysis to investigate the surface charge of the membranes, water contact angle to investigate the surface hydrophilicity/ hydrophobicity of the membranes, and x-ray photoelectron spectroscopy (XPS) to investigate the elemental composition of the membranes.

2.1.2 Equations

The rejection of NaCl and urea was calculated using equation (1). The standard flux and permeance model of equation (2) was used to calculate the water permeance of each test. The osmotic pressure of each solution was calculated using equation (3). The solute permeability for both NaCl and urea was calculated using equation (4).

$$R = 1 - \frac{C_p}{C_f} \quad (1)$$

$$J_w = A(\Delta P - \Delta\pi) \quad (2)$$

$$\pi = iCR_gT \quad (3)$$

$$J_s = J_w \times C_p \quad (4)$$

Where:

R = the rejection

C_p = the permeate concentration (mol/L)

C_f the feed concentration (mol/L)

J_w = the water flux (L/m^2/h or LMH)

A = the membrane water permeance (LMH/bar)

ΔP = the difference in pressure (bar) between the feed and permeate (atmospheric pressure, 0 barg)

$\Delta\pi$ = the difference in osmotic pressure (bar) between the retentate and permeate

i = the dissociation constant (2 for NaCl and 1 for urea)

C = the concentration of NaCl or urea (mol/L)

R_g = the universal gas constant (0.08314 L*bar/(mol*K))

T = the testing solution temperature (295 K)

J_s = the solute flux (mol/(m^2*h))

2.2 Project Facility/Physical Apparatus

2.2.1 Design Criteria

The purpose of this project was to improve the urea rejection of polyamide membranes. To ensure the membranes were still adequate for RO, we had set design criteria of pure water permeance of > 1 LMH/bar and > 95% NaCl rejection. That being said, we understand that it is likely the NaCl rejection could have been lower if we had a higher cross-linked membrane due to a significant reduction in free carboxylic acid groups, which are the dominant factor in the Donnan exclusion ability of RO membranes. Ultimately, our goal was to achieve a > 70% rejection for urea.

2.2.2 Source Water

We used the three water types in Table 1 to challenge our membranes. Note that these are simple laboratory solutions made with deionized water and not real environmental samples.

Table 1.—Summary of water types to challenge membranes

Water type	Component	Units[1]	Concentration
DI water	-----	-----	-----
Salt	NaCl	mg/L	2,000
Urea	Urea	mg/L	500

[1] mg/L = milligrams per liter.

2.2.3 Setup

We used a Sterlitech HP4750 dead-end stirred filtration cell (Sterlitech, USA) with a cell volume of 270 mL and an effective filtration area of 14.6 cm^2 for all membrane performance evaluation tests. Figure 6 shows the test cell used.

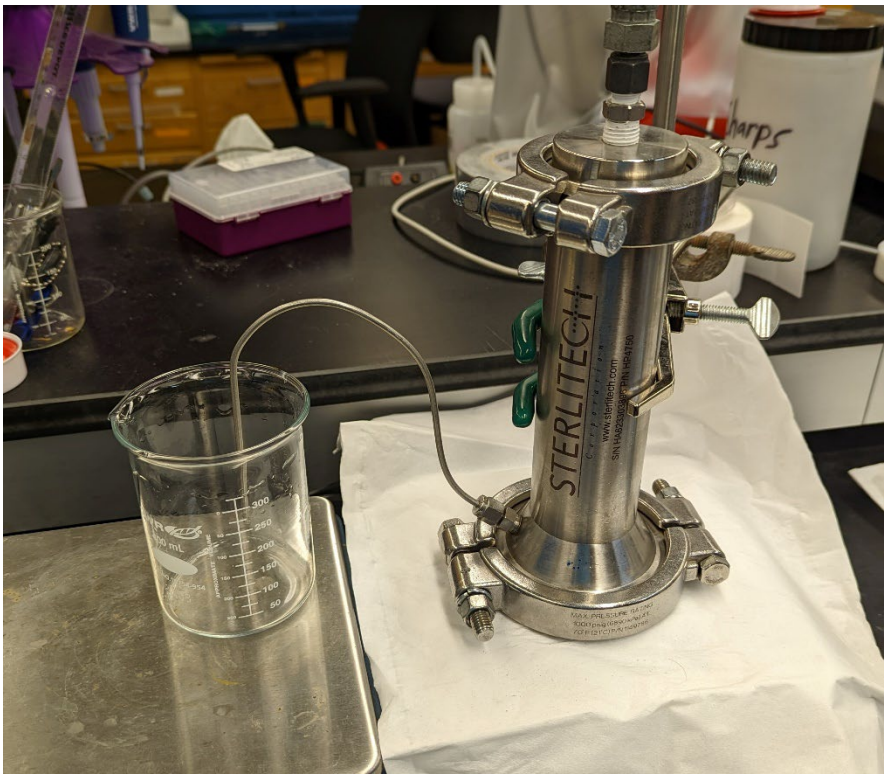

Figure 6.—Sterlitech test cell used to evaluate membrane performance.

2.3 Methodology

2.3.1 Methods Used

The majority of the methodology used can be found in (Habib and Weinman 2022). The methods used are described below.

2.3.1.1 *Materials*

Crystallized urea (ACS grade, ≥ 99%), β-(N-Morpholino) 2-morpholinoethanesulfonic acid (MES) buffer (anhydrous, ≥ 99%), 1,4-diaminobutane (DAB, ≥ 98%), (≥ 98%), PEI 600 and 10,000 g/mol molecular weight, and EDC (≥ 98%) were used as received from VWR®. DAP (≥ 99%), NaCl (≥99%), MPD (99%), and 4-(2-hydroxyethyl)piperazine-1-ethanesulfonic acid buffer (HEPES, ≥ 99.5%) were used as received from Sigma Aldrich (Millipore-Sigma). NHS (≥ 98%) and DAO (≥ 98%) were used as received from TCI Chemicals. Tricarballylic acid (99%) was used as received from Acros Organics. Thionyl chloride (≥ 99%) was used as received from Alfa Aesar. Aqueous solutions were made with deionized water from a Millipore Synergy ultraviolet (UV) water purification system. Commercial polyamide TFC RO membranes (XLE and BW30XFR) were kindly provided by Dupont Water Solutions. These membranes

consist of a polyester fabric backing, a polysulfone support layer, and a fully aromatic polyamide selective layer. The BW30XFR membrane has a coating on top of the polyamide layer while the XLE has no coating.

2.3.1.2 *Acid Chloride Synthesis*

The following protocol was used to convert tricarballylic acid into PTCA using thionyl chloride: (1) 2.205 g of tricarballylic acid was put into a round bottom flask with 25 mL of thionyl chloride; (2) Five drops of DMF was added to this mixture; (3) The flask was connected to a condenser and in a heating element set to 75 °C and run overnight; and (4) The flask was transferred to a distillation set up with the temperature controlled at 37 °C to remove the unreacted thionyl chloride. Distillation was performed until there was no longer any boiling.

2.3.1.3 *Membrane Synthesis*

Polyamide RO membranes were synthesized using the standard IP reaction methods. First, a Solecta PS20 membrane support was immersed in water overnight to remove any pore filler present. Then, the support membrane was removed from water and taped down to a glass square. A gasket was put around the edges of the membrane/glass plate and sealed with binder clips. The aqueous amine solution (generally 2 w/v% MPD or DAP) was poured onto the membrane and left for a designated time (generally 10 min). The aqueous solution was poured off the membrane, the gasket was removed, and the excess aqueous solution was removed via a rubber roller. A new gasket was installed, and the organic acid chloride solution (0.1-0.2 wt% TMC or PTCA in dodecane) was poured onto the membrane and left for 1 min. The organic solution was poured off the membrane, and the membrane was rinsed with hexane. The gasket was removed, and the membrane was immersed in water until used.

2.3.1.4 *Membrane Modification*

The XLE and BW30XFR membranes were provided as flat sheet rolls and stored dry until use. Before surface modification, each membrane was cut into circle coupons with an area of 19 cm^2 (a diameter of 4.92 cm^2) and immersed in deionized (DI) water overnight. Then 0.77 g of EDC, 0.115 g of NHS, and 2.922 g of NaCl were weighed on a ME403E precision balance (Mettler Toledo) and put into a 250-mL beaker. Then, 100 mL of aqueous 10 mM MES buffer solution was added to the beaker and stirred. The pH of the solution was adjusted to 5 using 0.1 M hydrochloric acid (HCl) and 0.1 M sodium hydroxide (NaOH). Next, the membrane coupon was put into the solution and placed on a VWR® Standard Analog Shaker for 4 h for activation of the carboxylic acid groups on the polyamide layer. After activation, the membrane was put into a 250-mL beaker with (0 w/v% or 2 w/v%) MPD, DAP, DAB, DAH, DAO, or PEI and 0.877 g NaCl in 100 mL of 10 mM HEPES buffer solution. The membrane was kept in the solution for 24 h at different temperatures (22 °C [room temperature], 47 °C [hot plate setting of 50 °C], 63 °C [hot plate setting of 80 °C], or 78 °C [hot plate setting of 95 °C]). To heat the solutions, a VWR® hot plate integrated with a temperature indicator was used. The membranes are discussed in Table 2 and Table 3. The control membranes are considered modified at 22 °C with no amine. *Note*: Data for the EDC-NHS activated only membranes are not included because the NHS half-life is on the order of minutes to hours depending on the physiological pH; therefore, it would not be a major factor in membrane property change.

Table 2.—Acronyms for XLE membranes

Membranes	EDC/NHS	Modification temperature	Amine
Control XLE (XLE-22)	Not used	22 °C	Not used
XLE-NHS-22-MPD	Used	22 °C	MPD
XLE-NHS-47-MPD	Used	47 °C	MPD
XLE-NHS-63-MPD	Used	63 °C	MPD
XLE-NHS-78-MPD	Used	78 °C	MPD
XLE-47	Not used	47 °C	Not used
XLE-63	Not used	63 °C	Not used
XLE-NHS-22-DAP	Used	22 °C	DAP
XLE-NHS-63-DAP	Used	63 °C	DAP
XLE-NHS-22-DAB	Used	22 °C	DAB
XLE-NHS-63-DAB	Used	63 °C	DAB
XLE-NHS-22-DAH	Used	22 °C	DAH
XLE-NHS-63-DAH	Used	63 °C	DAH
XLE-NHS-22-PEI (600)	Used	22 °C	PEI-600
XLE-NHS-63-PEI (600)	Used	63 °C	PEI-600
XLE-NHS-22-PEI (10K)	Used	22 °C	PEI-10,000
XLE-NHS-63-PEI (10K)	Used	63 °C	PEI-10,000

EDC = 1-(3 dimethylaminopropyl)-3-ethylcarbodiimide hydrochloride.
NHS = N-hydroxysuccinimide.
MPD = m-phenylenediamine.
DAP = 1,3-diaminopropane.
DAB = 1,4-diaminobutane.
DAH = 1,6-diaminohexane.
PEI = polyethenimine.

Table 3.—Acronyms for BW30 membranes

Membranes	EDC/NHS	Modification temperature	MPD
Control BW30 (BW30-22)	Not used	22 °C	Not used
BW30-NHS-22-MPD	Used	22 °C	Used
BW30-NHS-47-MPD	Used	47 °C	Used
BW30-NHS-63-MPD	Used	63 °C	Used
BW30-NHS-78-MPD	Used	78 °C	Used
BW30-47	Not used	47 °C	Not used
BW30-63	Not used	63 °C	Not used

EDC = 1-(3 dimethylaminopropyl)-3-ethylcarbodiimide hydrochloride.
NHS = N-hydroxysuccinimide.
MPD = m-phenylenediamine.

2.3.1.5 *ATR-FTIR*

ATR-FTIR was used to characterize the surface chemistry of the control and modified XLE and BW30XFR membranes. The measurements were done using a Perkin Elmer Spectrum 2 ATR-FTIR spectrometer equipped with a diamond ATR crystal in the range of 400–4,000 cm^{-1}. Data were processed by Spectrum 10 software. Each spectrum was collected for 32 scans at a resolution of 4 cm^{-1} and was baseline and ATR corrected with the Spectrum 10 software. All spectra were normalized to the peak at ≈1,490 cm^{-1}. A background of the ATR crystal was taken before each set of samples was tested to ensure the crystal was clean.

2.3.1.6 *SEM*

The control and modified XLE and BW30XFR membrane surface morphology were studied using an Apreo field emission scanning electron microscope (Thermo Fisher Scientific). The membrane samples were dried, attached with carbon tape to aluminum stabs, and sputter-coated with 12 nm of gold (MCM-200 ion sputter coater, SEC Co., Ltd., Korea) prior to SEM imaging. The SEM images were taken at an accelerating voltage of 5 kV, a current voltage of 50 pA, and a magnification of 10,000x.

2.3.1.7 *XPS*

XPS was used to analyze the elemental composition of the control and modified XLE and BW30XFR membranes. The XPS data were collected using a Phi Electronics Versaprobe 5000 with a monochromatic Al (1,486.6 eV) micro-focused source (100-µm spot size). The survey scans were taken with a pass energy of 187.85 eV, step size of 0.8 eV, and 25 ms time per step. Eight scans were taken per sample and averaged. The scans were analyzed using the Phi Multipak software. The elemental composition was obtained using the software's automatic identification and background subtraction, and the ratio of the area under the peak for nitrogen and oxygen was used to determine the nitrogen-to-oxygen (N/O) ratio of the sample.

2.3.1.8 *Static Contact Angle Goniometry*

Static water contact angles were measured on control and modified XLE and BW30XFR membrane samples to evaluate changes in hydrophilicity associated with the changes in surface chemistry. All static water contact angles were measured using the sessile drop method with a Dataphysics OCA-15EC contact angle analyzer. A liquid drop of deionized water (≈15 µL) was placed carefully on the sample surface. The sessile drop model was used in SCA 20 Analysis software to determine each contact angle. For consistency, measurements were taken 70 s after each water droplet was placed on the surface. Measurements were done at a minimum of nine locations on each sample to get an average contact angle value with standard deviation.

2.3.1.9 *Streaming Potential Analysis*

The zeta potential of the control and modified XLE and BW30XFR membrane surfaces were determined using an electrokinetic analyzer (SurPASS 3, Anton-Paar). Two membrane coupons were fixed to the sample holders of an adjustable gap cell with a gap size of 100 µm (sample size is 20 mm x 10 mm). In the experiment, an aqueous 0.01 M potassium chloride (KCl) solution was used as the measuring solution. For the pH adjustment, 0.05 M HCl and 0.05 M NaOH were used. The zeta potential was measured sequentially at pH 6, 9, and 3. The zeta potential was computed using the SurPASS 3 software using the Helmholtz-Smoluchowski equation. Measurements were done a minimum of three times to get an average zeta potential value with standard deviation.

2.3.2 Runs and Experiments Done

The water permeance and NaCl rejection of control and modified XLE and BW30XFR membranes were measured using a Sterlitech HP4750 dead-end stirred filtration cell (Sterlitech, USA) with a cell volume of 270 mL and an effective filtration area of 14.6 cm^2. The filtration cell was pressurized with nitrogen gas to a pressure of 230 psi. Each membrane was challenged with a DI water solution, a 2,000-ppm NaCl solution, and a 500-ppm urea solution. Each membrane was allowed to permeate for 30 min to allow for compaction before the permeate was collected on a ME403E precision balance (Mettler Toledo). At least 8 g of permeate was collected while recording the time to calculate the flux through the membrane. At least three membranes were tested for each membrane type for statistical relevance. The NaCl rejection was calculated by measuring the conductivity of the feed and permeate solutions using a VWR® Traceable Bench/Portable Conductivity Meter. The urea rejection was calculated by measuring the urea concentration of the feed and permeate using a HACH DR6000 UV-Vis Laboratory Spectrophotometer at a 195-nm wavelength using quartz cuvettes (VWR®). A calibration curve was constructed to calculate the urea concentration. Each sample was diluted two times using DI water because the calibration curve started to deviate from linear above 400 ppm. The flux of each membrane was calculated by dividing the permeate flow rate by the membrane testable area. For deionized water experiments, the flux was divided by the pressure difference (ΔP) to calculate the pure water permeance. For salt and urea rejection experiments, the flux was divided by ($\Delta P - \Delta \pi$) to calculate the water permeance.

3.0 Results and Discussion

3.1 Results

3.1.1 RO Membrane Synthesis Review Paper

We first surveyed the literature to determine the most common synthesis parameters when fabricating MPD-TMC based polyamide membranes. The results of this review can be found in (Habib and Weinman 2021). While there is no one consistent way to make RO membranes on the lab scale, we found using 2 wt% MPD in the aqueous solution, contacting the MPD solution on a polysulfone support membrane for 2 min, removing the MPD solution from the support using a rubber roller or an air knife, contacting the MPD-soaked membrane with a 0.1 wt% TMC in n-hexane solution for 0.5 min, and heat curing in an oven at 75 °C for 10 min to be the most common parameters used. Additives generally improve the resulting membrane performance. The main challenge with synthesizing RO membranes is that different labs will use the same or very similar synthesis conditions but end up with very different results, indicating polyamide RO membrane synthesis is as much of an art as it is a science.

3.1.2 RO Membrane Support Layer Properties Review Paper

We also surveyed the literature to determine the effect of support layer properties on the IP reaction and, consequently, on the polyamide selective layer performance. We highlighted the significance of selective layer-support layer connectivity on the properties of TFC membranes (Mokarizadeh et al. 2021). Our search suggests that there are still inconsistencies among the results reported in the literature. There are studies about the impact of support layer pore size, porosity, and hydrophilicity on selective layer properties; however, the conclusions seemed to be divergent in nature, proving that there is a need for more investigation on this topic. Moreover, the synergistic effect between properties of the support layer, such as the simultaneous effect of pore size and hydrophilicity on the selective layer, should be investigated.

3.1.3 RO Membrane Control

The first thing we had to do was synthesize an adequate polyamide membrane with the standard MPD- and TMC-based chemistry so we could compare our new chemistries. We spent a significant amount of time figuring out what worked best for us. We spoke with numerous industrial and academic experts in RO membrane synthesis to help us figure out how to make better membranes. We eventually settled on 2 wt% MPD on 20 kDa polysulfone membrane (Solecta PS20) for 10 min, remove with rubber roller, 0.1–0.2 wt% TMC in dodecane for 1 min, no curing. This membrane ultimately gave us a water permeance of 1.4 LMH/bar and a NaCl rejection of 95%.

3.1.4 New Chemistries

3.1.4.1 *DAP*

We tried many tests to use DAP as a replacement for the MPD monomer (middle row of Figure 4). Our thoughts behind this were the flexibility of DAP compared to MPD would lead to tighter membranes capable of rejecting urea at a higher level. We tried many synthesis approaches to get performing membranes, including (1) using DAP as the monomer, (2) using DAP as a co-monomer with MPD, (3) using DAP as an additive with MPD, (4) using various soaking procedures, and (5) adjusting the monomer solution pH to ensure no DAP ionization in the aqueous phase. However, none of these tests resulted in good salt-rejecting membranes (all < 75% NaCl rejection with most < 40%). Additionally, we performed SEM on these membranes and found that the membranes appeared more like nanofiltration membranes with smooth and nodular features instead of the rough, ridge-and-valley like structures common to RO membranes. These results led us to stop using DAP.

3.1.4.2 *PTCA*

Next, we tried making membranes using PTCA as a replacement for the TMC monomer (bottom row of Figure 4). An industrial expert suggested that MPD is the best amine monomer for RO membranes, and our time would be better spent on finding alternatives to the acid chloride monomer. We made PTCA by converting 1,2,3-propanetricarboxylic acid into the acid chloride version using thionyl chloride. We chose PTCA because some simple computational simulations performed by Dr. Heath Turner's group at The University of Alabama showed that the MPD-TMC network pore size is ≈0.35 nm, while the MPD-PTCA is ≈0.18 nm. Urea is ≈0.36 nm in diameter, so getting to 0.18 nm would make rejection simpler; however, the PTCA monomer also did not produce good membranes. The best urea rejection we could get with PTCA alone was 3.5% and, when mixed with TMC, 23%, which is lower than our standard MPD-TMC based membrane.

3.1.5 Polyamide Membrane Modification

3.1.5.1 *MPD Modification*

First, we will discuss the results from modifying polyamide RO membranes with MPD. These results can be found in (Habib and Weinman 2022). To conjugate MPD with the polyamide layer, EDC was used to activate the free carboxylic acid groups of the polyamide layer. EDC reacts with the carboxylic acid groups and forms an unstable O-acylisourea intermediate. To form a more stable intermediate, NHS was used. The EDC couples the carboxyl acid groups with NHS and forms a dry-stable NHS-ester intermediate. Lastly, the NHS-ester intermediate couples the carboxyl acid groups with MPD, forming a new polyamide bond, which was confirmed by the ATR-FTIR and XPS data. Figure 7A shows the ATR-FTIR spectra of the control and modified XLE membranes. Each membrane showed characteristic peaks at ≈1,660 cm^{-1}, ≈1,610 cm^{-1}, and ≈1,540 cm^{-1}, representing the amide I band, aromatic amide band, and amide II band of a fully aromatic polyamide layer, respectively. Membranes modified using MPD did not

exhibit any shifts or changes in peak position compared to the control; however, the MPD modified membranes showed a slightly more intense amide I band peak, a more intense aromatic amide band peak, and a more intense amide II bond peak. When the heat was introduced along with employing the MPD to the modification process, the peak intensity was found to be increased further. We suspected the addition of heat increased the rate of reaction between MPD and activated carboxylic groups, causing more MPD molecules to react to the membrane surface; however, the peak intensity did not increase monotonically with an increase in the modification temperature, indicating the reaction rate on the membrane surface did not increase linearly with temperature. Figure 7B shows the ATR-FTIR spectra of control and modified BW30XFR membranes. Similar to the control and modified XLE membranes, the BW30XFR membranes also showed the key peaks at the same wavelengths, and an increase in the peak intensity was observed with the extent of modification. To understand the effect of MPD on the modification at high temperatures, both the XLE and BW30XFR membranes were modified at 47, 63, and 78 °C without using MPD, and in both cases, the peak intensity was found to be similar compared to the controls (Figure 7C and D). Thus, the increase in the intensity of these peaks indicated the presence of more amide groups on the polyamide separation layer, which mostly happened due to the introduction of MPD.

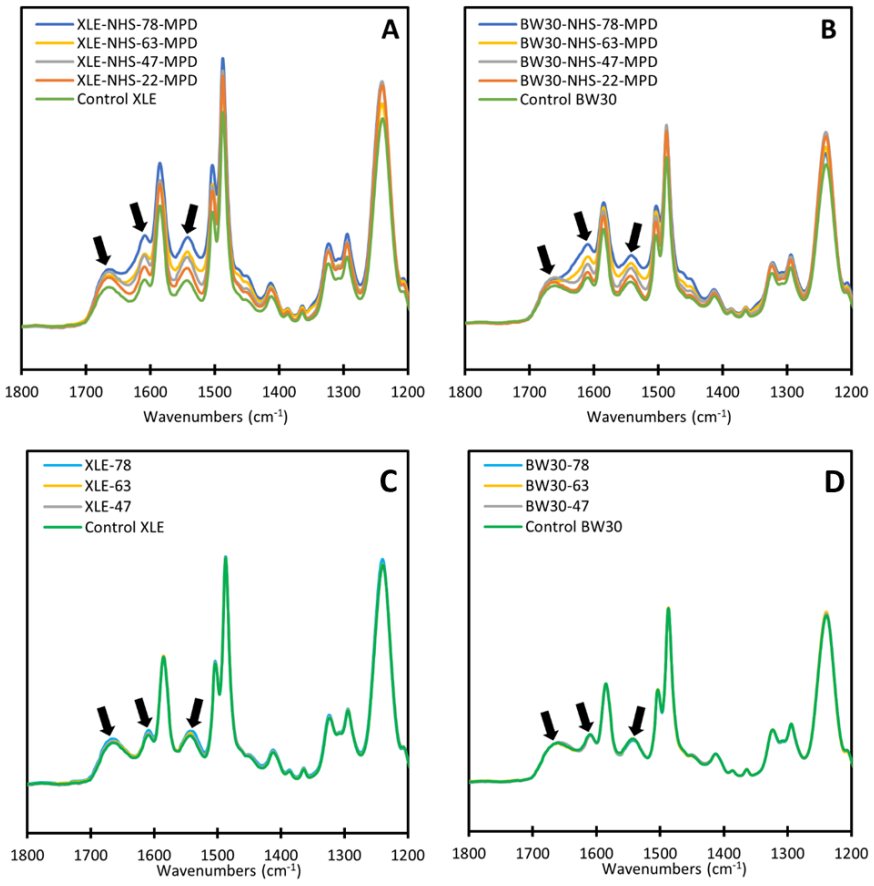

Figure 7.—ATR-FTIR spectra of XLE and BW30 membranes.

To determine whether the surface morphology changed with temperature and/or MPD modification, SEM imaging of the XLE and BW30XFR membranes was performed for both control and modified membranes. The surface morphology was found to be the same for all membranes. Both control and modified membranes exhibited a ridge-and-valley structure with no apparent change. Even if any changes have occurred, it likely happened at the angstrom-scale, which requires advanced characterization techniques like positron annihilation lifetime spectroscopy (PALS) to detect.

The control and modified XLE and BW30XFR membranes were further characterized by XPS. Table 4 shows the data obtained from the XPS characterization. As each MPD molecule possesses two nitrogen atoms and no oxygen atoms, the membranes after modification should have a larger N/O ratio than the control membranes because one oxygen atom is removed for the addition of two nitrogen atoms. The amount of MPD added to the membrane surfaces is unlikely to significantly change the amount of C present in the whole polyamide layer thickness measured by XPS, which is seen in Table 4. We are only modifying the membrane surfaces; it is highly unlikely that the EDC-NHS activators penetrate the cross-linked polyamide layers. Compared to the control XLE membranes, the N/O ratio of modified XLE membranes had a statistical increase when the modification was done using MPD at room temperature. The N/O ratio increased with an increase of the modification temperature, indicating more MPD on the polyamide layer. In the case of BW30XFR membranes, the N/O ratio of BW30-NHS-22-MPD, BW30-NHS-47-MPD, BW30-NHS-63-MPD, and BW30-NHS-78-MPD did not change statistically compared to the control. The extent of MPD modification was not very apparent due to the more cross-linked and tighter network structure of BW30XFR membranes; however, the average values for the BW30-NHS-63-MPD and BW30-NHS-78-MPD membranes were higher than the control BW30XFR membrane, just with a larger variance, suggesting more modification with MPD happened at 63 and 78 °C.

Table 4.—XPS data of XLE and BW30 membranes

Membrane	C	N	O	N/O ratio
Control XLE	74.84 ± 0.53	10.77 ± 0.63	14.39 ± 0.23	0.75 ± 0.05
XLE-NHS-22-MPD	73.94 ± 0.49	14.16 ± 0.58	11.90 ± 0.15	1.19 ± 0.06
XLE-NHS-47-MPD	73.10 ± 1.31	14.53 ± 0.78	12.38 ± 1.09	1.18 ± 0.12
XLE-NHS-63-MPD	74.60 ± 1.74	14.86 ± 0.77	10.54 ± 1.28	1.42 ± 0.15
XLE-NHS-78-MPD	73.97 ± 1.82	15.61 ± 1.07	10.42 ± 0.86	1.50 ± 0.07
Control BW30	73.70 ± 0.40	12.88 ± 0.36	13.42 ± 0.77	0.96 ± 0.08
BW30-NHS-22-MPD	74.75 ± 0.08	12.58 ± 0.16	12.68 ± 0.08	0.99 ± 0.02
BW30-NHS-47-MPD	73.53 ± 1.47	12.93 ± 1.01	13.54 ± 1.41	0.96 ± 0.15
BW30-NHS-63-MPD	72.60 ± 1.18	14.96 ± 0.93	12.43 ± 1.68	1.22 ± 0.20
BW30-NHS-78-MPD	71.94 ± 2.93	14.77 ± 1.39	13.30 ± 2.85	1.16 ± 0.30

To understand the effect of the modification on the hydrophobicity of the XLE and BW30XFR membranes, static water contact angle measurements were performed. Figure 8A and 8B show the water contact angle data for the XLE and BW30XFR membranes. Compared to the control XLE and BW30XFR membranes, the MPD modified membranes exhibited a statistical increase in water contact angle, which indicates an increased hydrophobicity of the polyamide layer. The increase in the water contact angle is believed to happen due to the binding of MPD to the NHS-activated surface, which decreased the amount of hydrophilic carboxylic acid moieties and increased the amount of hydrophobic aromatic rings. We suspected that with more MPD attachment there would be more amine-water hydrophilic interactions and less aromatic ring-water hydrophobic interactions, keeping the water contact angle approximately the same for the all the XLE and BW30XFR MPD-modified membranes.

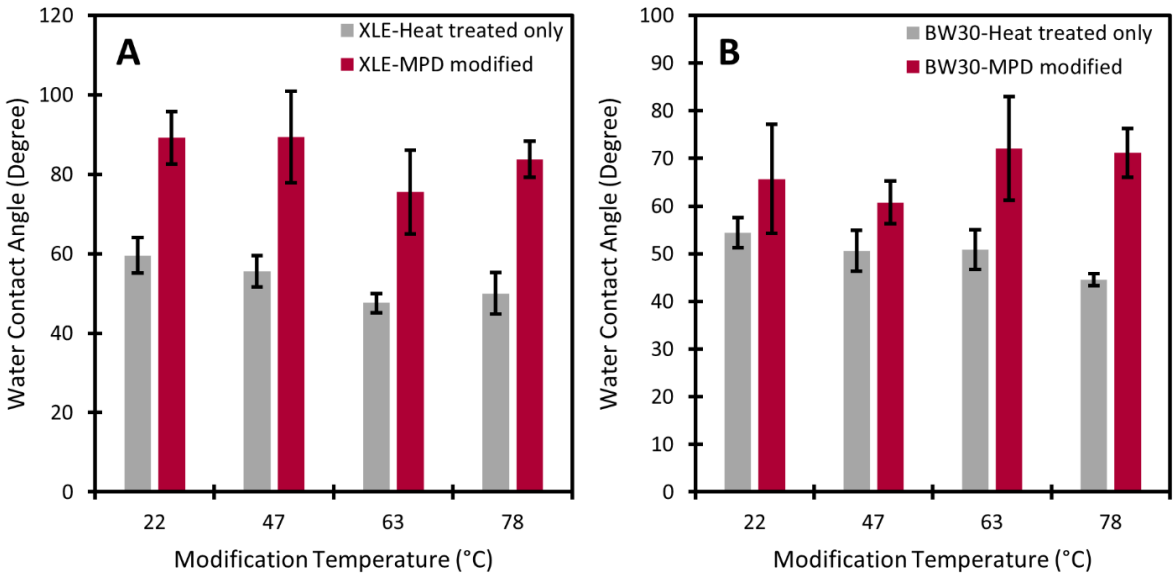

Figure 8.—Water contact angle of XLE and BW30 membranes.

To investigate the effect of MPD modification on membrane surface charge, the zeta potential of each membrane was measured at pH 9, 6, and 3 as shown on Figure 9A and 9B. The surface charge of the control and modified XLE membranes were positive at pH 3. The XLE membrane modified with MPD at all temperatures exhibited a higher positive surface charge at pH 3 than the control XLE membrane. In the case of pH 6, all the XLE membranes showed a negative surface charge, with the control XLE membrane showing the most negative surface charge and the XLE membrane modified at 78 °C with MPD showing the least negative surface charge. The zeta potential of the modified XLE membranes also was found to be increased at pH 9 compared to the control XLE membrane. The phenomenon of less negative surface charge for modified XLE membranes at pH 9 can be attributed to the increased positive charge density of the protonated amine groups from the newly incorporated MPD molecules and a decrease in the

deprotonated carboxylic acid groups. Similar to XLE membranes, the zeta potential of the modified BW30XFR membranes exhibited a higher positive surface charge compared to the control BW30XFR at pH 3. The modified BW30XFR membranes also showed an increase in zeta potential value with increasing modification temperatures at pH 6. For the zeta potential values at pH 9, except for the BW30-NHS-22-MPD membrane, all the modified BW30XFR membranes showed a higher zeta potential than the control membrane. When we compared the zeta potential of Control XLE, XLE-47, XLE-63, and XLE-78, we observed a similar or slight change in zeta potential at pH 3, pH 6, and pH 9 (Figure 9C). In the case of the BW30XFR membranes (Figure 9D), Control BW30, BW30-47, BW30-NHS-63, and BW30-78 membranes exhibited similar or slight changes in zeta potential at pH 3, pH 6, and pH 9.

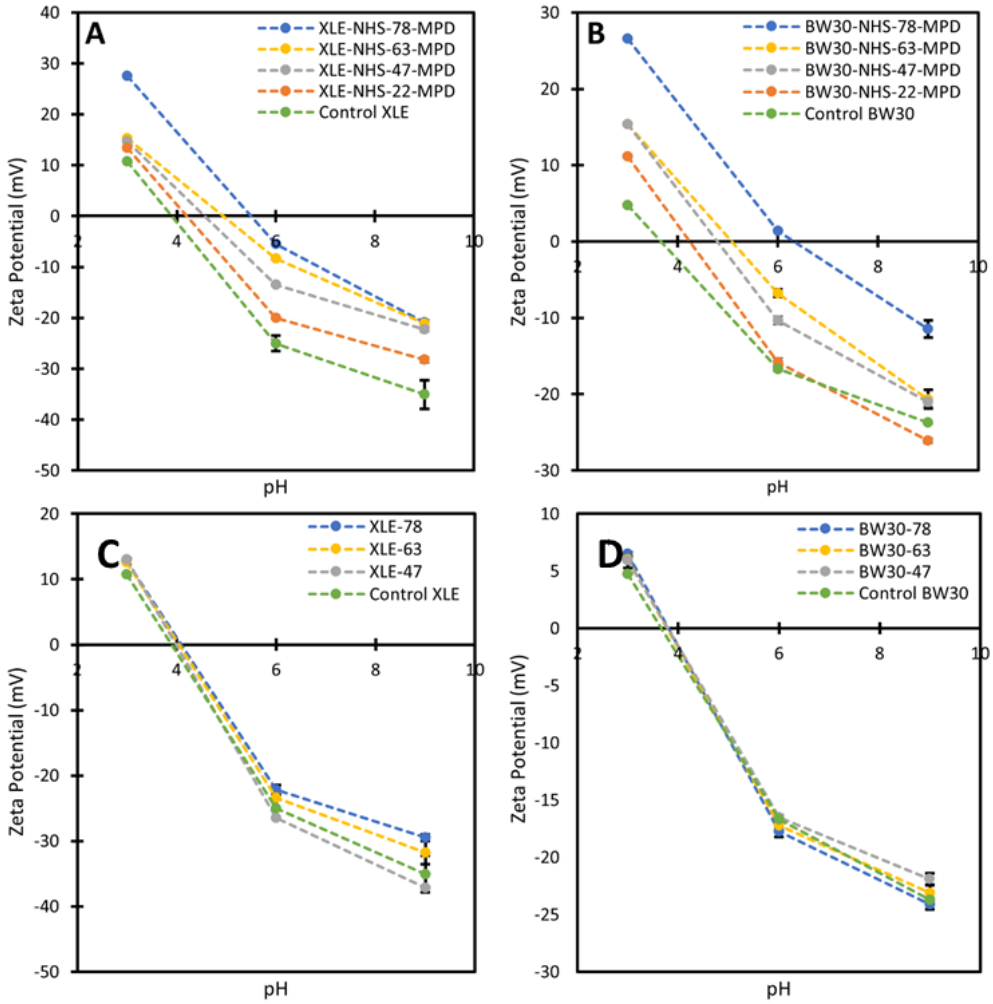

Figure 9.—Zeta potential of XLE and BW30 membranes.

Membrane performance, including pure water permeance, NaCl rejection, and urea rejection, were measured for both XLE and BW30XFR membranes. For both XLE and BW30XFR membranes, the modified membranes exhibited a statistical decrease in pure water permeance compared to their respective control membranes with the increase in the modification temperature. This may be attributed to the reduction in the free volume due to the increased coupling of MPD and/or rearrangement of the pores due to heat treatment. Figure 10 shows the membrane performance results for the XLE membranes when challenged with NaCl and urea solutions. Figure 10A show the water permeance and NaCl rejection for the control and modified XLE membranes. As the experiment was performed using a dead-end stirred cell setup and some extent of concentration polarization possibly happened, the NaCl rejection of all the XLE membranes was lower than the manufacturer's provided value (97%), where a crossflow setup was used. The NaCl rejection of the membranes modified with MPD at room temperature (22 °C) and 47 °C were found to be statistically similar to the control XLE. The heat-treated only XLE membranes exhibited similar NaCl rejection compared to the control XLE membrane; however, in the case of XLE-NHS-63-MPD and XLE-NHS-78-MPD, the NaCl rejection had a statistical decrease. Also, the NaCl rejection for the XLE-NHS-63-MPD and XLE-NHS-78-MPD membranes were statistically different from their heat-modified counterparts. The decrease in the NaCl rejection at higher temperatures can be explained by the reduction of the Donnan charge exclusion effect. At higher temperatures, more MPD molecules reacted with the activated carboxylic acid groups, forming a polyamide bond, and reducing the available negatively charged moieties to reject the chloride ions of NaCl. The decrease in the negative charge, and likely the free volume, of the polyamide layer also affected the water permeance of the XLE membranes. The control XLE membrane had an average water permeance of 7.95 ± 0.57 $L/m^2/h/bar$. All of the modified XLE membranes had a statistical decrease in water permeance compared to the control XLE membrane. XLE membranes modified using MPD at 22 , 47, 63, and 78 °C had an average water permeance of 5.30 ± 0.19, 4.20 ± 0.16, 3.46 ± 0.01 and 1.98 ± 0.42 $L/m^2/h/bar$, respectively. For the heat-treated membranes, their water permeance values were lower than the control XLE membrane but higher than their MPD-modified counterparts. Compared to the control XLE membrane, the MPD-modified XLE membranes exhibited lower water permeance likely due to the tighter structure, pore rearrangement, and increased hydrophobicity, and the heat-treated XLE membranes exhibited lower water permeance likely due to pore rearrangement. Figure 10B shows the water permeance and urea rejection of the control XLE and modified XLE membranes. Similar to the NaCl rejection tests, the water permeance had a statistical decrease with an increase in the modification temperature. In the case of urea rejection for the XLE membranes, the urea rejection was found to be increased from 16.8 to 36.3% when the XLE membrane was modified with MPD at room temperature (22 °C) compared to the control XLE membrane. Unlike the NaCl rejection, the modified XLE membranes showed a continuous increase of urea rejection with increasing modification temperature. The urea rejection of XLE-NHS-47-MPD, XLE-NHS-63-MPD, and XLE-NHS-78-MPD membranes had a statistical increase up to 46.3, 54.4, and 54.9%, respectively, when compared with control XLE. The increase in urea rejection at high temperatures is likely attributed to the reduction of the free volume of the polyamide layer by both MPD attachment and pore rearrangement from the hot water bath.

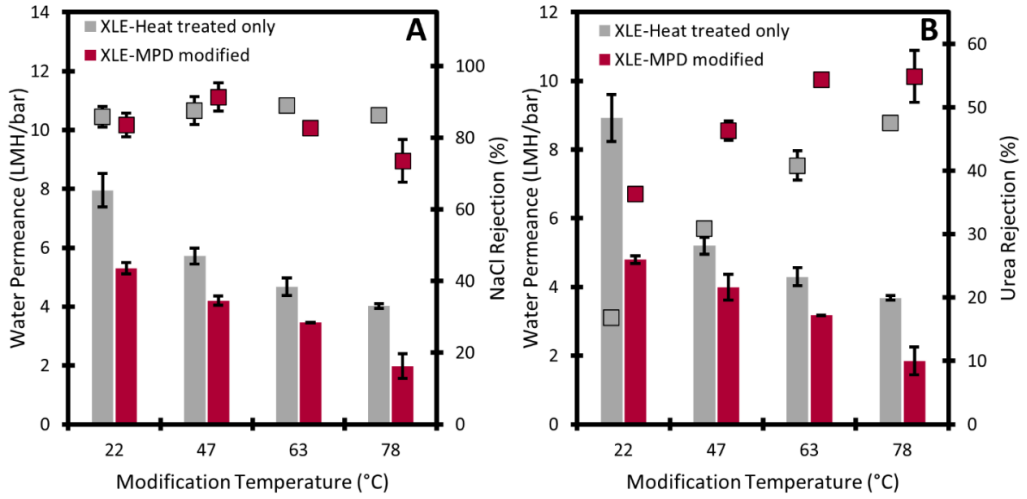

Figure 10.—Water permeance, NaCl rejection, and urea rejection of XLE membranes.

Figure 11 represents the membrane performance data of the BW30XFR membranes when challenged with NaCl and urea solutions. Figure 11A shows the water permeance and NaCl rejection for the control and modified BW30XFR membranes, respectively. The BW30XFR NaCl rejection was found to follow the same trend exhibited by the XLE membranes. Modifying the BW30XFR membranes at room temperature (22 °C) did not change the NaCl rejection statistically compared to the control BW30 membrane, but when the modification temperature was 63 and 78 °C, the NaCl rejection had a statistical decrease. There was a statistical increase in the urea rejection and decrease in water permeance when the modification temperature of the BW30XFR membrane was increased, which is shown on Figure 11B. Compared to the control BW30XFR, the urea rejection of BW30-NHS-22-MPD, BW30-NHS-47-MPD, BW30-NHS-63-MPD, and BW30-NHS-78-MPD were increased up to 54.1, 56.6, 59.4, and 61.3%, respectively; however, the magnitude of the change in urea rejection between the control BW30XFR and the modified BW30XFR membranes was smaller than the change between the control XLE and the modified XLE membranes. This can be explained by the presence of a more cross-linked polyamide layer of the BW30XFR membrane compared to the less cross-linked polyamide layer of the XLE membrane.

To understand the role of heat treatment in the modification and its effect on the urea rejection, both the XLE and BW30XFR membranes were modified at 22, 47, 63, and 78 °C using 0% MPD. In the case of the XLE membranes, when XLE-NHS-22-MPD and control XLE (which we considered as XLE-22) were compared, the urea rejection was found to be statistically increased for the XLE-NHS-22-MPD, which is shown on Figure 10B. Similarly, the presence of MPD increased the urea rejection of the XLE-NHS-47-MPD, XLE-NHS-63-MPD, and XLE-NHS-78-MPD membranes when compared to their heat-treated counterparts, XLE-47, XLE-63, and XLE-78; however, the urea rejection of the modified XLE membrane using 0% MPD at 47, 63, and 78 °C had a statistical increase compared to the control XLE membrane, which indicates not only MPD, but also heat, played an important role in improving the urea rejection of XLE membranes.

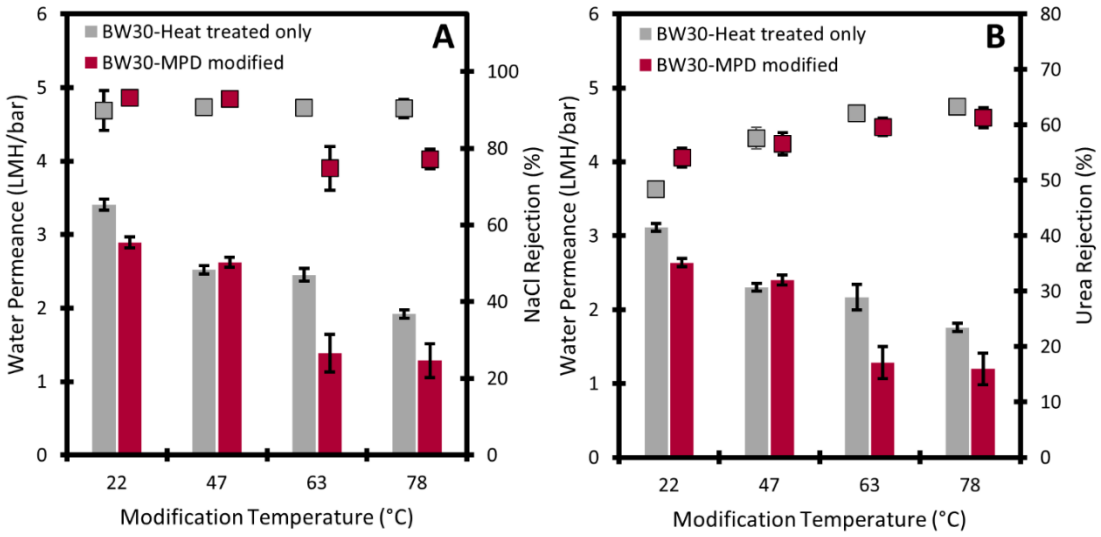

Figure 11.—Water permeance, NaCl rejection, and urea rejection of BW30 membranes.

The BW30XFR membranes modified with 2% MPD at 22 °C exhibited improved urea rejection compared to the control BW30XFR membrane, which is shown on Figure 11B. Interestingly, when we compared the BW30-NHS-47-MPD, BW30-NHS-63-MPD and BW30-NHS-78-MPD membranes with BW30-47, BW30-63 and BW30-78, we observed similar urea rejection. When the modification temperature was at 47 °C or higher, the heat played a more crucial role than the MPD. Because of the application of heat, it is likely the pores were narrowed, which decreased the free volume of the polyamide layer and increased urea rejection. On the other hand, as the polyamide layer of the BW30XFR membrane was denser and had a lower number of free carboxylic acid groups available, the MPD failed to significantly contribute to improved urea rejection. The commercial coating on the polyamide layer of the BW30XFR membrane also may have played a crucial role in preventing the MPD from modifying the polyamide layer significantly; however, the BW30XFR membranes modified without MPD at different temperatures showed higher water permeance compared to the BW30XFR membranes modified using MPD. Even though there was an increase in urea rejection for the MPD modified XLE and BW30XFR membranes, a 1.9–4.7-fold and a 1.2–2.7-fold decrease in pure water permeance was observed compared to the control XLE and BW30XFR membranes.

Lastly, we calculated the NaCl and urea solute permeability to get a better understanding of the solute transport through the membrane. Figures 12A–D show the results. When we compared the NaCl solute permeability of the control XLE and XLE-NHS-22-MPD membranes, we observed a higher NaCl solute permeability for the control XLE membrane. At higher temperatures, the membranes showed similar NaCl solute permeability regardless of whether MPD was used or not. In the case of control BW30 and modified BW30 membranes, the NaCl solute permeabilities were statistically the same even though the XLE and BW30 membranes that were modified with MPD at higher temperatures (63 and 78 °C) showed lower water permeance, which could decrease the NaCl solute permeability. The lower NaCl rejection of these membranes is likely

due to the absence of repulsion charges from the carboxylic acid groups increased the NaCl permeability; however, urea solute permeability was statistically decreased when the XLE membranes were modified with MPD at 22, 47, 63, and 78 °C. The heat-treated XLE membranes showed higher urea solute permeability compared to their MPD-modified counterparts but was lower than the control XLE membrane. We suspect the mechanism of improved urea rejection with heat treatment is due to the thermal rearrangement of the polyamide layer, which needs to be investigated with PALS measurements. The combination of a higher water flux and lower urea rejection for the heat-treated membranes lead to this significant difference in urea solute permeability. In the case of BW30 membranes, except the BW30-47 membrane, the urea solute permeability was higher for the heat-treated only membranes compared to their MPD-modified counterparts. The BW30-NHS-47-MPD membrane and the BW30-47 membrane showed similar urea solute permeability, as both showed almost same water permeance and urea rejection.

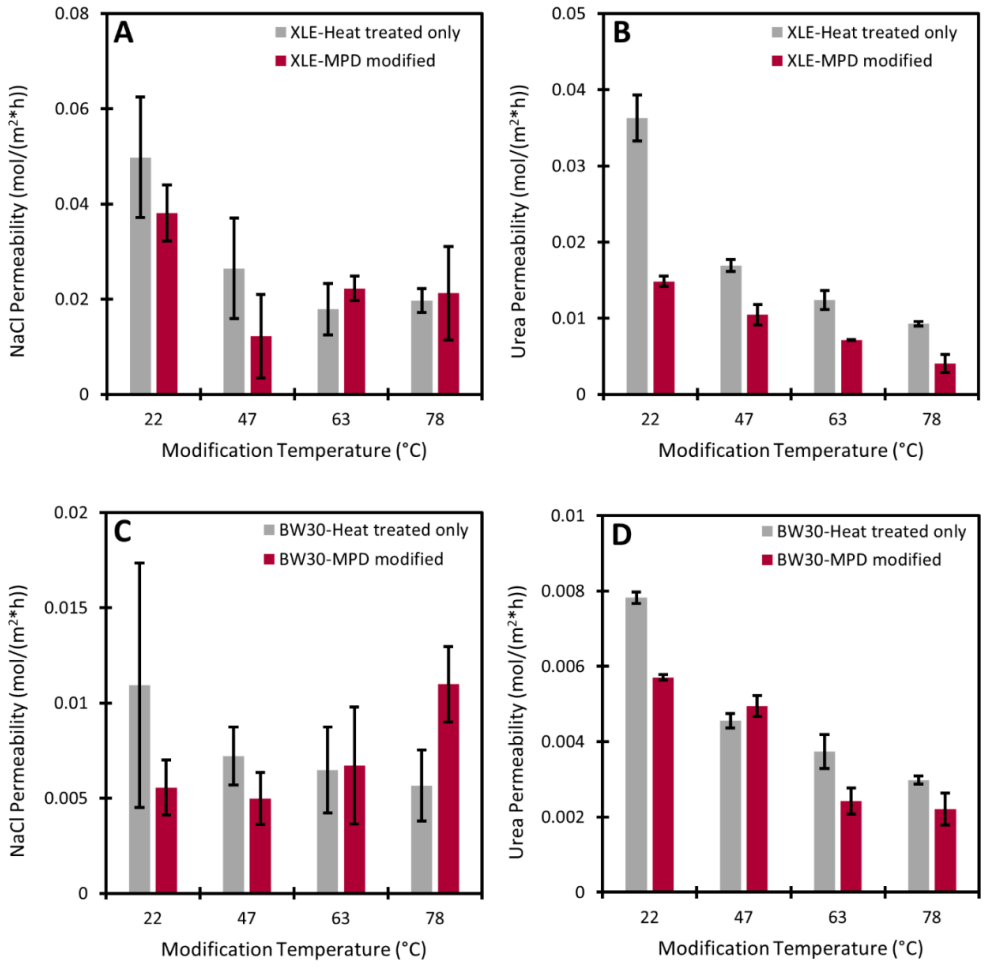

Figure 12.—NaCl and urea solute permeability of XLE and BW30 membranes.

3.1.5.2 *Linear Diamine Modification*

After activation of the XLE membrane surface with carbodiimide chemistry, the activated carboxylic acid of the NHS-ester intermediate couples with DAP, DAB, or DAH, forming a new polyamide bond. The formation of this bond was confirmed by the ATR-FTIR data. Figure 13 shows the ATR-FTIR spectra of the control and modified XLE membranes. The increase in the peaks in the aliphatic -CH2- stretching region of 2,800–3,000 cm^{-1} confirms the conjugation of the linear diamines with the free carboxylic acid groups on the membrane. The XLE-NHS-22-DAH membrane exhibited the greatest aliphatic stretching. This is expected due to the greater number of C-H bonds in DAH compared to DAP and DAB. The control XLE and XLE-63 membranes exhibited the lowest -CH2- stretching because they were not modified with aliphatic amines and, therefore, had the fewest number of C-H bonds. It can also be observed that membranes modified at room temperature exhibited greater stretching than membranes modified with heat, which suggests the thermal rearrangement of the polyamide layer may in some way inhibit the coupling of diamines to the free carboxylic acid groups on the polyamide layer.

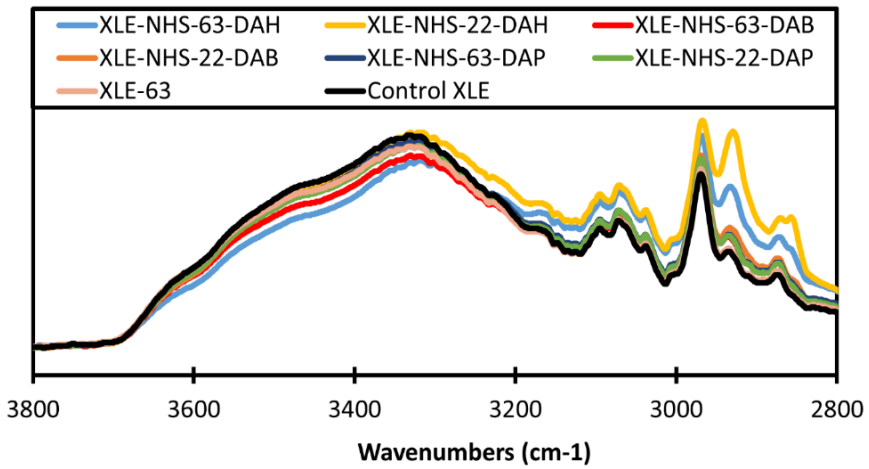

Figure 13.—ATR-FTIR spectra of linear amine modified XLE membranes.

Membrane performance was tested for pure water permeance, salt rejection, and urea rejection for both the control and the modified XLE membranes. It was determined via statistical analysis that the pure water permeance of each of the modified XLE membranes was statistically different and significantly lower than that of the control XLE membrane. The significant decrease in pure water permeance between the control and modified XLE membranes could be explained by improved cross-linking and a likely decrease in the free volume hole size within the polyamide layer via amine coupling and/or thermal rearrangement. The ability of the control and modified XLE membranes to reject NaCl is displayed on Figure 14. The average NaCl rejection of the control XLE membrane was found to be 86.5%. This value is lower than the expected value of 97% provided by the manufacturer. It is probable that this difference in the NaCl rejection of the control XLE membrane can be attributed to concentration polarization consistent with dead-end filtration, which is not seen in less sensitive cross-flow filtration. A statistical analysis revealed

that the salt rejection for the XLE-63, XLE-NHS-22-DAP, XLE-NHS-63-DAP, XLE-NHS-22-DAB, XLE-NHS-63-DAB, and XLE-NHS-22-DAH membranes were statistically similar to the control XLE membrane. Conversely, it was determined that only the XLE-NHS-63-DAH membrane NaCl rejection was statistically different from and higher than that of the control XLE membrane. Based on the Donnan Exclusion effect, we would expect the salt rejection of the modified XLE membranes to decrease from that of the control XLE membrane because, by reacting the free carboxylic acid groups, we are decreasing the negative charge on the surface of the membrane; however, the overall maintenance or improvement of the NaCl rejection for the modified XLE membranes as compared to the control XLE membrane suggests that replacing this negative charge with positively charged amine groups that can extend away from the membrane surface is just as sufficient or better in reference to the charge exclusion properties of the membrane. This demonstrates that the modified XLE membranes are still sufficient for the rejection of salt from water.

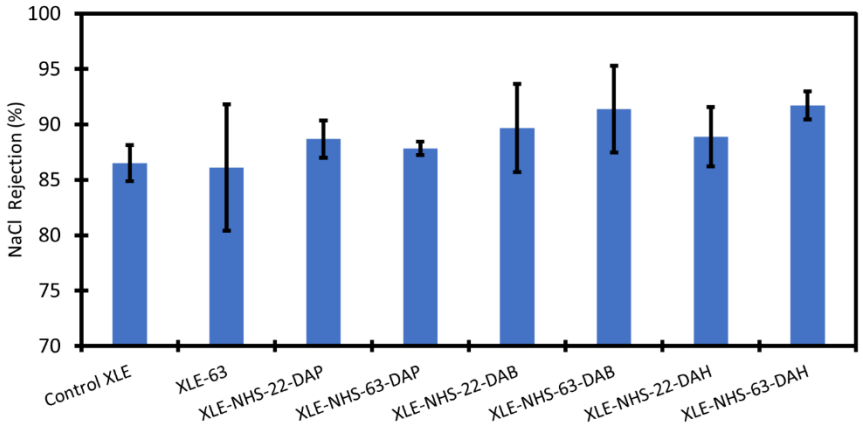

Figure 14.—NaCl rejection of linear-amine modified XLE membranes.

The rejection of urea for the control and modified XLE membranes is depicted on Figure 15. It was determined via statistical analysis that the urea rejections of the XLE-63, XLE-NHS-63-DAP, XLE-NHS-22-DAB, XLE-NHS-63-DAB, XLE-NHS-22-DAH, and XLE-NHS-63-DAH membranes were statistically different and significantly higher than that of the control XLE membrane. It was found that only the urea rejection of the XLE-NHS-22-DAP membrane was statistically similar to that of the control XLE membrane. The significant increase in urea rejection for the modified membranes demonstrates that both diamine coupling (except for DAP) and thermal rearrangement improve the ability of the XLE membrane to reject urea. The average urea rejection of each of the membranes modified at 63 °C was higher than that of their 22 °C counterparts; furthermore, the XLE-63 modified membrane exhibited the greatest average urea rejection of all the membranes tested. It was determined via statistical analysis that the urea rejection of the XLE-63 membrane was statistically different and higher than that of the XLE-NHS-63-DAB membrane but statistically similar to that of the XLE-NHS-63-DAH and

the XLE-NHS-63-DAP membranes, which suggests that the thermal rearrangement of the polyamide layer is a greater determining factor in the ability of the modified XLE membranes to reject urea than linear diamine coupling.

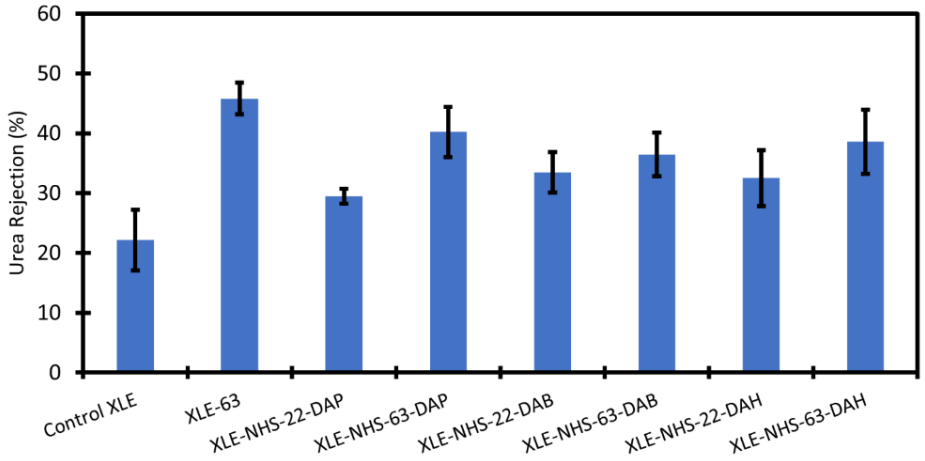

Figure 15.—Urea rejection of linear-amine modified XLE membranes.

Next, we tested new modification techniques to further improve urea rejection performance. First, we split up the amine modification and heating steps. When we did this using MPD modification, we found we could get a membrane with a higher water permeance (2.5 LMH/bar), NaCl rejection (89.6%), and urea rejection (58.7%) than when combing these methods. With DAO as the amine modifier, we were got a lower water permeance (1.0 LMH/bar) but higher NaCl (93.1%) and urea (61.2%) rejections. Lastly, we began investigating the use of a microwave to perform the heating step to reduce the length of each experiment. For the XLE membrane only heated using a microwave for 1.5 min (no amine modification), the urea rejection increased to 49.0%. When using the microwave for 1.5 min instead of heating for 24 h with DAO modification, the urea rejection increased by 4% to 65.3%. This strategy is promising, and we will continue to investigate.

3.1.5.3 *Polyamine Modification*

Next, we modified the XLE membrane with two polyamines of the same chemical, PEI, but different molecular weights (600 and 10,000 g/mol). The results are shown on Figure 16. The results shows that combining heat and PEI significantly improves the urea rejection; however, it is not higher than the MPD-modified membranes.

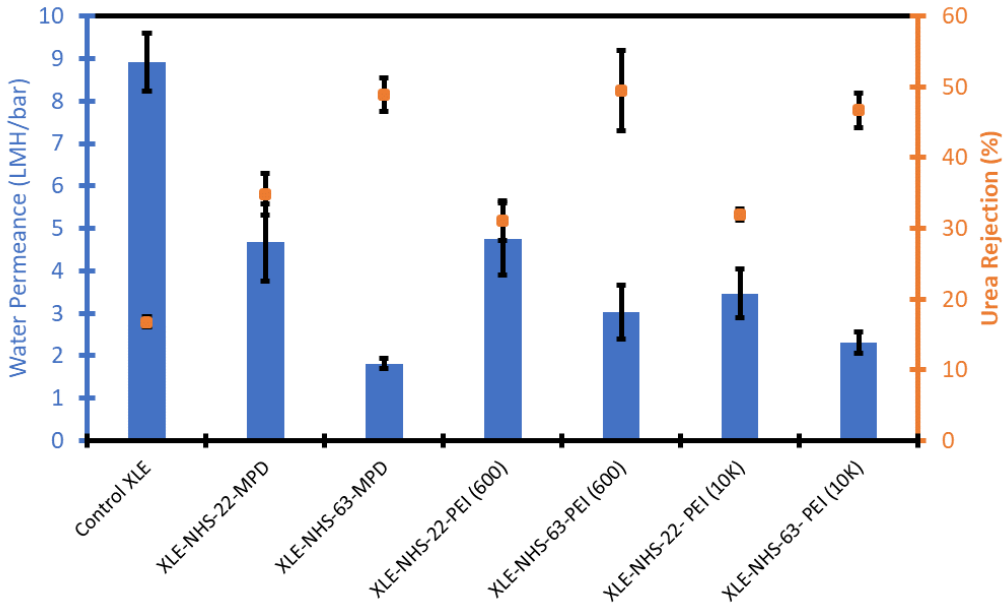

Figure 16.—Water permeance and urea rejection of modified XLE membranes.

3.2 Analysis

3.2.1 New Chemistries

Unfortunately, none of the new chemistries we used made a successful membrane. We believe this is due to the fragility of the layers that were formed and that the network pores in simple molecular dynamics simulations wanted to fold upon themselves. These might make decent nanofiltration membranes, but they would not make good membranes for rejecting NaCl, urea, and other small, neutral molecules. Thinking this might be due to the totally linear structure of the DAP and PTCA monomers, we investigated using other chemistries that contain rings, such as 3,3′,5,5′-tetracarboxydiphenylmethane; however, the addition of a single methylene group connecting the rings together, which appeared in simple molecule drawings to give a smaller network pore size, led to instability in the network pore in the molecular dynamics simulations.

3.2.2 Amine Modification

A method was developed for combining chemical modification and heat treatment of commercial XLE and BW30XFR membranes to enhance the rejection of urea. For the chemical modification, carbodiimide chemistry was used followed by the coupling of MPD. The chemical modification of the commercial membranes was performed at room temperature (≈22 °C) and higher temperatures (47–78 °C), whereas the control XLE and BW30XFR membranes had an average urea rejection of 16.8 and 48.4%, respectively, the modified XLE and BW30 membranes had a

36.3–54.9% and 54.1–64.6% urea rejection depending on the modification temperature and percentage of MPD applied during the post-modification. These results supported our hypothesis. The increase in urea rejection of the modified XLE membranes was attributed mainly to the employment of MPD in the post-modification stage, whereas the increase in urea rejection for the modified BW30XFR membranes was attributed to the hot water bath treatment. The control XLE membrane had an average urea rejection of 22.1%, and the modified XLE membranes had a 29.5–45.8% average urea rejection depending on the diamine used and whether the membrane was subjected to heat treatment; however, in the case of both membranes, the water permeance was reduced significantly, although this is to be expected if the free volume hole size is reduced. Using linear diamines and separating the modification and heating steps is leading to urea rejections > 60%; however, this data is still preliminary and must be substantiated.

4.0 Conclusions

4.1 New Chemistries

New chemistries need to be developed to produce polyamide RO membranes that are capable of rejecting small, neutral molecules like urea; however, none of the linear chemistries used in this project produced a good membrane. Even when investigating other chemistries with significantly more ring rigidity, the addition of a single methylene group capable of rotating leads to instability in the network pore structure. New chemistries must produce rigid network pores of a smaller size than the MPD-TMC chemistry.

4.2 Amine Modification

Combining chemical modification and heat treatment of commercial RO membranes can significantly enhance the small, neutral molecule rejection. We believe this is attributed to a reduction in the free volume hole size. By splitting up the modification step and the heating steps, the urea rejection was further increased. More work needs to be done to verify the mechanism of enhanced urea rejection. Additionally, there is a need to understand whether the modification increases the degree of crosslinking and/or if it just fills in the aggregate pores.

4.3 Challenges

Polyamide RO membrane synthesis is incredibly challenging. We have found it to be more of an art than a science. To understand if these synthesis and modification strategies are valid, one needs to have the basics of IP down to perfection. While we were able to achieve 95% NaCl rejection, we would prefer that number to be closer to 99%. Utilizing the expertise from industry and experts within the field would be necessary to implement these strategies, both at the reproducible lab scale and at the pilot and commercial scales. The modification strategy developed presents additional challenges for scale-up, as the process may take multiple days. We are attempting to reduce part of the time by using a microwave, but it is unclear how microwave heating can be scaled up in a roll-to-roll process. It would be helpful to have a new method developed for activating carboxylic acid bonds that does not take as long as carbodiimide chemistry. Additionally, the carbodiimide chemistry only activates the polyamide membrane surface, not the internal structure. It would be beneficial if we could modify the entire polyamide layer by utilizing chemistries that can diffuse into the membrane.

4.4 Recommended Next Steps

New chemistries need to be synthesized and utilized that produce smaller network pores than the conventional MPD-TMC membrane. While this may lead to a reduction in water permeance, a significant enhancement in selectivity is worth it for these challenging separations. It is recommended to investigate rigid-ring-based structures that do not significantly deform when relaxed. The use of computational simulations such as molecular dynamics simulations can provide useful information about the stability of the network pores before any experiments are done.

Ongoing work involves exploring alternative chemical modification strategies, including other diamines of varying lengths and structures. More investigation is needed into the effect of heat treatment on the membranes, especially since there is no visual difference in the membrane surface and morphology upon modification. It is crucial to quantify the free volume hole size changes using the different modification techniques by using PALS measurements. PALS can offer the fundamental insights needed to understand what is happening to the membranes at the Angstrom scale. Ultimately, for the modification strategy to be implemented at a pilot or commercial scale, the modification time needs to be significantly reduced.

Another alternative is membrane surface functionalization using adsorptive additives such as metal organic frameworks (MOFs). The development of adsorptive membranes with selectivity toward urea will enhance the removal of urea from water. Ongoing work involves exploring the grafting of Fe-MOF on the surface of polyamide membranes for the adsorption of urea during water filtration.

5.0 References

Ananiev, A.V., J.-C. Broudic, and P. Brossard. 2003. The urea decomposition in the process of the heterogeneous catalytic denitration of nitric acid solutions: Part I. Kinetics of the reaction. *Applied Catalysis B: Environmental* 45 (3):189–196. https://doi.org/10.1016/S0926-860X(03)00236-9

Bogard, M.J., D.B. Donald, K. Finlay, and P.R. Leavitt. 2012. Distribution and regulation of urea in lakes of central North America. *Freshwater Biology* 57 (6):1277–1292. https://doi.org/10.1111/j.1365-2427.2012.02775.x

Finlay, K., A. Patoine, D.B. Donald, M.J. Bogard, and P.R. Leavitt. 2010. Experimental evidence that pollution with urea can degrade water quality in phosphorus-rich lakes of the Northern Great Plains. *Limnology and Oceanography* 55 (3):1213–1230. https://doi.org/10.4319/lo.2010.55.3.1213

Glibert, P.M., J. Harrison, C. Heil, and S. Seitzinger. 2006. Escalating Worldwide use of Urea – A Global Change Contributing to Coastal Eutrophication. *Biogeochemistry* 77:441–463. https://doi.org/10.1007/s10533-005-3070-5

_____. 2021. A review on the synthesis of fully aromatic polyamide reverse osmosis membranes. *Desalination* 502:114939. https://doi.org/10.1016/j.desal.2021.114939

Habib, S. and S.T. Weinman. 2022. Modification of polyamide reverse osmosis membranes for the separation of urea. *Journal of Membrane Science* 655:120584. https://doi.org/10.1016/j.memsci.2022.120584

Liu, J., X. Chen, Z. Shao, and P. Zhou. 2003. Preparation and characterization of chitosan/Cu(II) affinity membrane for urea adsorption. *Journal of Applied Polymer Science* 90 (4):1108–1112. https://doi.org/10.1002/app.12841

Mokarizadeh, H., S. Moayedfard, M.S. Maleh, S.I.G.P. Mohamed, S. Nejati, and M.R. Esfahani. 2021. The role of support layer properties on the fabrication and performance of thin-film composite membranes: The significance of selective layer-support layer connectivity. *Separation and Purification Technology* 278:119451. https://doi.org/10.1016/j.seppur.2021.119451

Rahimpour, M.R. and H.R. Mottaghi. 2009. Simultaneous Removal of Urea, Ammonia, and Carbon Dioxide from Industrial Wastewater Using a Thermal Hydrolyzer−Separator Loop. *Industrial & Engineering Chemistry Research* 48 (22):10037–10046. https://doi.org/10.1021/ie900751g

Schnetzer, A., P.E. Miller, R.A. Schaffner, B.A. Stauffer, B.H. Jones, S.B. Weisberg, P.M. DiGiacomo, W.M. Berelson, and D.A. Caron. 2007. Blooms of *Pseudo-nitzschia* and domoic acid in the San Pedro Channel and Los Angeles harbor areas of the Southern California Bight, 2003–2004. *Harmful Algae* 6 (3):372–387. https://doi.org/10.1016/j.hal.2006.11.004

Yoon, Y. and R.M. Leuptow. 2005. Removal of organic contaminants by RO and NF membranes. *Journal of Membrane Science* 261(1-2):76–86. https://doi.org/10.1016/j.memsci.2005.03.038